The Dynamics of Green Spaces and their Heat Island Cooling Effect in Guangzhou

Xiaohan Xie*

Suzhou Innovation Academy, Suzhou, 215131, China

* Corresponding Author Email: Ruby.Xie.2027@sia-edu.cn

Abstract. Urban green spaces play a key role on mitigating surface urban heat island (SUHI). This study used Guangzhou China as the research region, based on multi-temporal LANDSAT remote sensing images from 2006 to 2025, the spatiotemporal evolution characteristics of urban green spaces were analyzed, and the cooling effect of this product on SUHI was quantitatively evaluated too. The result shows that the total area of urban green spaces was stable, while the spatial pattern tends to be fragmented. High-temperature areas were mainly distributed in the southern built-up area of the study region, and low-temperature areas were scattered in patches in the north. Besides, the average temperature in green areas is significantly lower than that in non-green areas, and significant differences were found among independent samples of green spaces temperature and non-green spaces temperature($P<0.001$). Relevant analysis shows, there is a negative correlation between green space area and surface temperature ($r=-0.282$), but the linear model has a low fit. The study found that area contributes to cooling, while spatial configuration and landscape connectivity also significantly influence the cooling effect, and the distribution of urban heat islands is closely related to the fragmentation and spatial pattern of green spaces. The findings of this study can provide observational clues and basic data for subsequent more complex quantitative analyses.

Keywords: Urban green space, Urban heat island, Surface temperature, Cooling effect.

1. Introduction

The urbanization process is accelerating. According to United Nations' statistics on global urban populations, until 2050, the proportion of the world's urban population will increase from 56% in 2021 to 68% [1]. To adapt to the rapid development of society, the structure and positioning of cities have changed, and they have begun to expand the area of their functional zones, and improve their basic public facilities, resulting the continuous destruction and encroachment of green spaces in cities and certain evolutionary patterns have emerged. This phenomenon exacerbates the urban thermal environment [2].

Global climate varies by region, the most prominent of these is the increasingly severe urban heat island phenomenon. The Urban Heat Island (UHI) phenomenon, where urban temperatures are significantly higher than in surrounding rural areas, along with heat waves, has become one of the greatest social threats to the well-being, production, daily life, and health of modern people [3-5]. Guangzhou is a typical example, where rapid growth in population and building density has led to a decrease in green space and intensified the UHI effect. Numerous studies have analyzed the urban heat island effect in Guangzhou, for example, Su Yongxian et al. selected 17 sample points within the study area and conducted a quantitative study on the temperature distribution pattern around urban parks using remote sensing images, finding that the temperature difference between the park's perimeter and the boundary points is positively correlated with the distance from the park. Fan Yapeng et al. used multi-time series satellite remote sensing data from 1990 to 2008 to calculate the NDVI and IBI building indices, discussed their relationship with the urban thermal environment, and obtained the expansion trend of the urban heat island [6-8]. Therefore, exploring the evolution of green spaces and their heat mitigation effects in Guangzhou is of great significance.

This study uses Google Earth Engine to acquire and process remote sensing data, extracting green space and surface temperature. It uses the equal interval and mean-standard deviation methods to analyze the spatial distribution of urban heat islands and quantify the heat mitigation benefits of green

spaces. This research aims to reveal the relationship between spatial pattern and mitigation effect, providing relevant departments with a basis for spatial planning and decision-making.

2. Data Collection and Methods

2.1. Data Sources and Processing

Considering the large amount of long-term (2006-2025) image data and the unified processing involving multiple sensors. The entire data acquisition and processing workflow of this study was completed on the Google Earth Engine (GEE) platform [13-15]. GEE, an online globalization processing engine, integrates preprocessing algorithms for Landsat series data such as radiometric calibration, atmospheric correction, and cloud masking. Taking into account data availability and urban development processes, 2006 was selected as the starting point with four-year intervals covering Landsat 5/8/9 data from 2006 to 2025. The specific years are 2006, 2010, 2014, 2018, 2022, and 2025, and the data sources are detailed in Table 1. It is worth noting the 2026 Landsat imagery was only updated to May 24th and could not represent the summer conditions. Therefore, 2025 with complete data, was used as the study endpoint.

Additionally, data products used in this study have been radiometrically calibrated by the USGS, with atmospheric and geometric corrections based on the LaSRC algorithm. Hence, data preprocessing only included image screening (cloud cover <30%), cloud masking, and boundary cropping to Guangzhou boundary.

Table 1. The Sources of Data

Data identification	Satellite parameters	Time	Sensor	Resolution	Band Number
LANDSAT/LC09/C02/T1_L2	Landsat 9	2022.1.1-2022.12.31 2026.1.1-2026.5.22	OLI/TIRS	30m	7
LANDSAT/LC08/C02/T1_L2	Landsat 8	2014.1.1-2014.12.31 2018.1.1-2018.12.31	OLI/TIRS	30m	7
LANDSAT/LT05/C02/T1_L2	Landsat 5	2006.1.1-2006.12.31 2010.1.1-2010.12.31	TM	30m	7

2.2. Study Methods

The NDVI threshold method (NDVI > 0.25) is used for quick extraction of green spaces across wide ranges due to its simplicity and operational convenience. By calculating NDVI and vegetation cover FVC through multispectral bands, it estimates the emissivity, then combining the brightness temperature from the thermal infrared sensor to achieve LST inversion, thereby supporting subsequent SUHI and buffer analysis.

In practice, this article adopts USGS Landsat Collection2 Level-2(L2) Surface temperature products. The near-infrared band units are converted to degrees Celsius in GEE, with the annual LST raster derived from the 12-month average temperature.

Besides, the mean-standard deviation method divides LST into six temperature levels to characterize range and aggregation of SUHI. To intuitively analyze and find the effective cooling range, buffer zones are used to calculate the cooling effect at different distances.

Further, this study will compare LST differences between green spaces and non-green spaces through t-test, while Pearson correlation analysis quantifies the linear relationship between the proportion of green space and LST quickly to measure the mitigation effect of green spaces. Finally, green space, SUHI distribution, and LST difference comparison map will be generated to analyze the cooling effect.

3. Result and Analysis

3.1. Green Spaces Distribution and Changes

Related studies have shown that urban green spaces can effectively mitigate the green space effect through tree canopy shading, vegetation transpiration, and water evaporation [9]. According to data, except a sharp decrease in 2010 and a significant increase in 2014, the overall green space area in Guangzhou has remained relatively stable at around 6,000 km². The data anomalies for these two consecutive years may be due to the limited number of satellite images in the study period and region resulting from cloud cover filtering, leading to missing data and thus displaying abnormal data. Besides, the outliers could also be due to misjudgment caused by NDVI threshold classification when processing mixed pixels. According to statistics from the GEE, the total area of green space in Guangzhou was 6,059.47 in 2006, and will reach 5,948.35 km2 by 2025. The overall area of green space decreased by only about 111.12 km2 during the study period. However, Fig 1 shows the urban landscape pattern has undergone significant changes, mainly manifested in increased fragmentation. In terms of spatial distribution, the green space in the northern part of the study area is distributed in large patches with strong overall connectivity. While the cities are mainly distributed in the southern part of the study area. Within the urban area, green spaces exhibit obvious point-like and fragmented distribution characteristics, and their area is constantly being encroached upon by the urban built-up area. Fragmentation is a key factor affecting the urban heat island effect, and reduced connectivity of green spaces within cities will greatly weaken the cooling effect of green spaces.

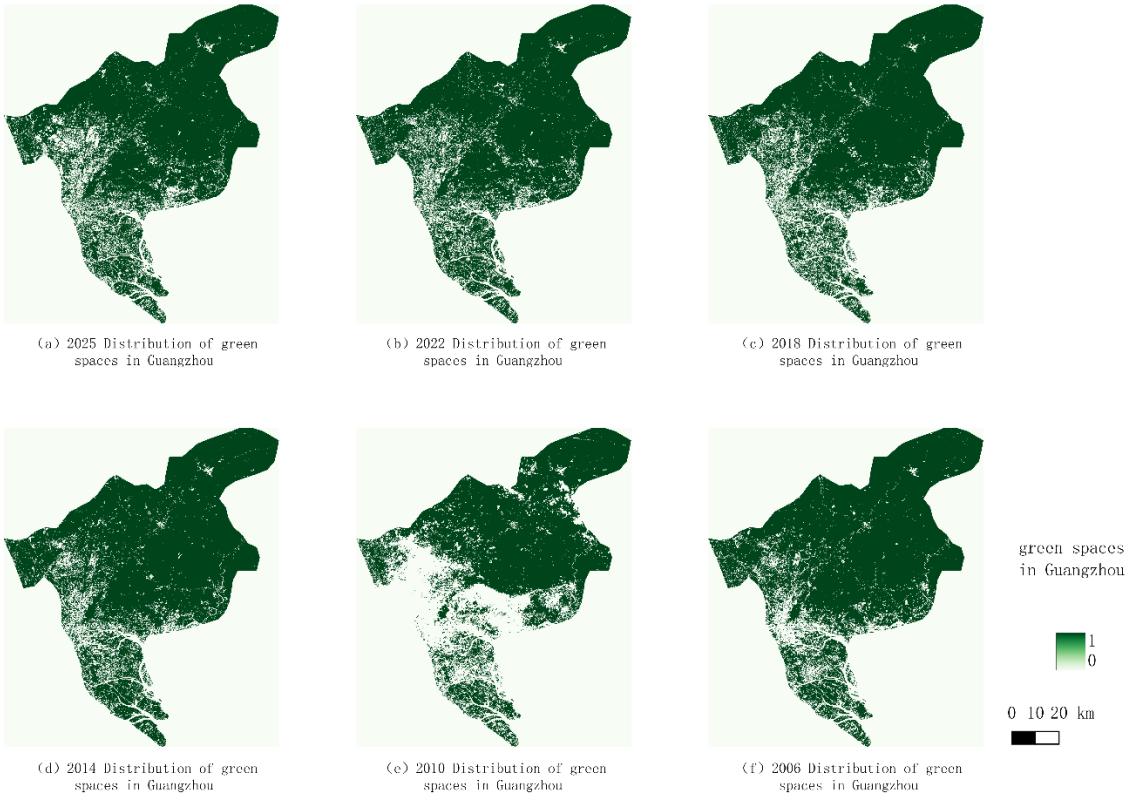


Fig. 1 Spatiotemporal distribution of green spaces in Guangzhou

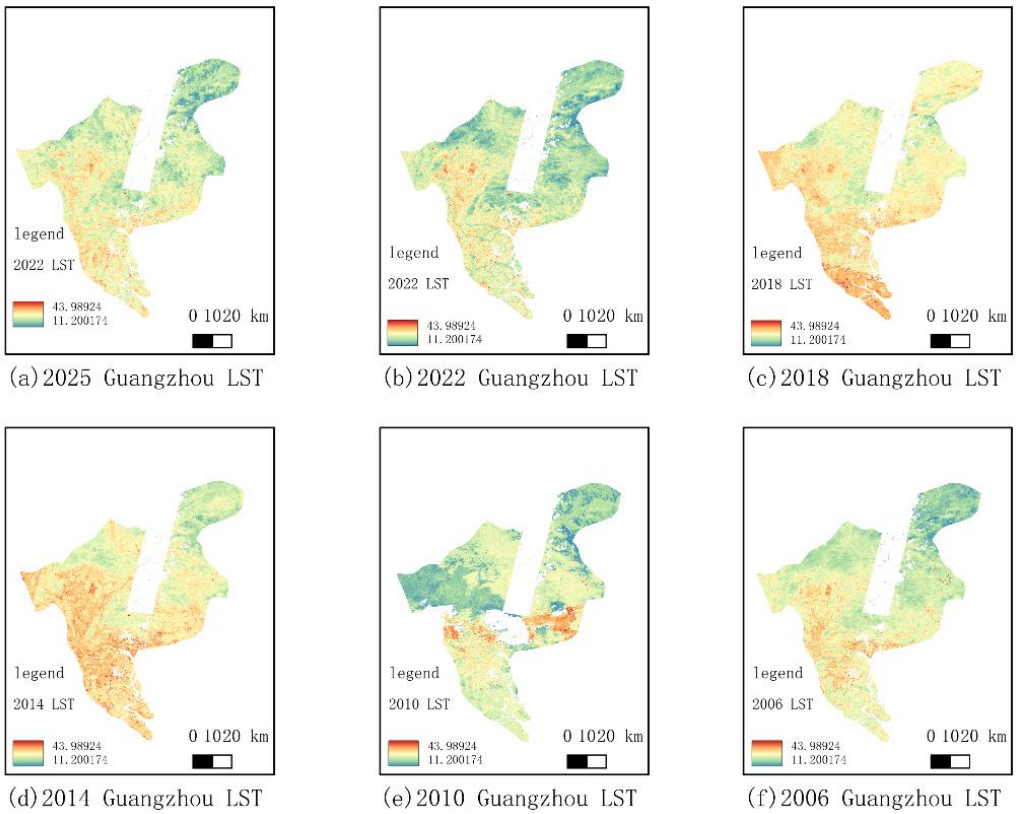
3.2. Spatial Distribution of LST and SUHI

To visually represent the surface temperature distribution in the study area, this study uses a surface temperature map (LST) to reflect the temperature situation across Guangzhou. Referring to the research on green space and heat island effect in Nanchang City by Liu Guangliang, Huang Zixuan and others [10], the surface temperature of Guangzhou City was divided into six different temperature levels, which is extra high, high, second high, medium, low and cold area, by using the mean-standard deviation method. To directly present the spatial distribution characteristics of temperature levels, a

surface urban heat island distribution map (SUHI) will be generated. The SUHI classification criteria are shown in Table 2 (where μ is the mean and σ is the standard deviation).

Table 2. SUHI temperature classification standard

Level	Temperature range (Based on μ and σ)
Extra high	$T \geq \mu + 2\sigma$
High	$\mu + \sigma \leq T < \mu + 2\sigma$
Second high	$\mu \leq T < \mu + \sigma$
Medium	$\mu - \sigma \leq T < \mu$
Low	$\mu - 2\sigma \leq T < \mu - \sigma$
Cold	$T < \mu - 2\sigma$



(a) 2025 Guangzhou LST (b) 2022 Guangzhou LST (c) 2018 Guangzhou LST

(d) 2014 Guangzhou LST (e) 2010 Guangzhou LST (f) 2006 Guangzhou LST

Fig. 2 Guangzhou LST distribution

As can be seen from the LST image shown in Fig 2, the medium and high temperature areas represented by red and yellow in the figure mainly coincide with the urban built-up areas in the south, while the low temperature areas represented by blue and green are mainly concentrated in the patchy green spaces in the north. From 2006 to 2015, the average temperature reached its highest point in 2022, at approximately 31℃, then declining to 25℃ by 2025. Compared to 2006, the overall decline was approximately 3℃. In terms of time series, the area of high-temperature regions shows a trend of first expanding and then contracting. During the study period, the high-temperature area continued to spread from the south to the north and surrounding areas, reaching its maximum coverage between 2014 and 2018, with some high-temperature patches even encroaching on the northern region. After 2018, the high-temperature zone has shrunk significantly, and by 2025 it will have shrunk back to the southern built-up area. The low-temperature zone, on the other hand, is characterized by high fragmentation and poor connectivity, and its area has shrunk over time.

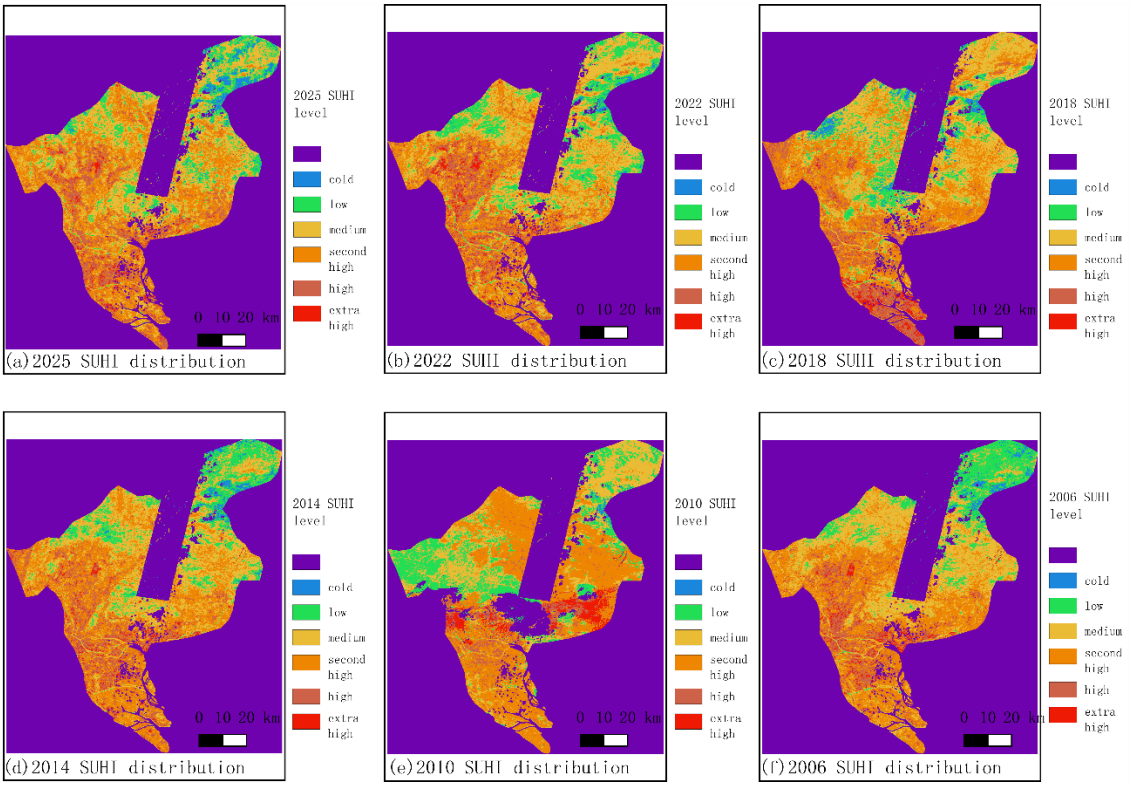


Fig. 3 Guangzhou SUHI distribution

As can be seen from the heat island intensity map in Fig 3, there are obvious north-south differences in the surface urban heat island (SUHI), and the high-temperature zone overlaps significantly with the urban built-up area. Between 2006 and 2025, the spatial distribution of the heat island shows strong stability, and the range and location of the high-temperature zone have not shifted drastically. In contrast, the low-temperature areas are smaller and mainly concentrated in the northern part of the study area. They have fragmented over time and exhibit a scattered distribution pattern.

3.3. Cooling Effect of Green Spaces

3.3.1. Comparison between Green Spaces and Non-green Spaces with LST

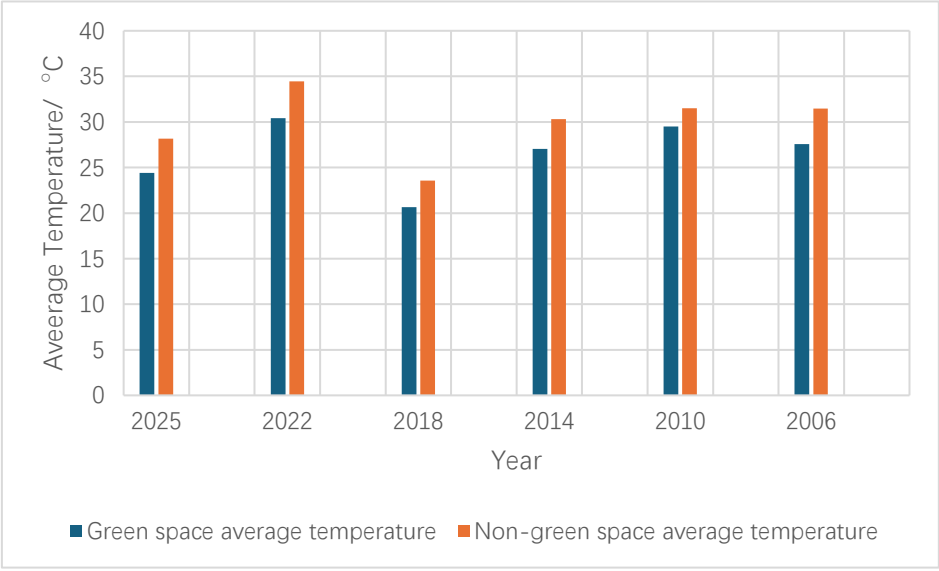


Fig. 4 Bar chart of Average Temperature in Green and Non-green Areas

As can be seen from the comparison of the average temperature of green areas and non-green areas in Fig 4, green areas have a significant cooling effect. From 2006 to 2025, independent samples t-tests showed that the surface temperature of green areas was significantly lower than that of non-

green areas, with a statistically significant difference (P<0.001), and the temperature difference between the two remained stable at around 4 degrees Celsius. Meanwhile, except for 2010, the standard deviation of temperature in green areas remained stable at around 3.5, while the standard deviation of temperature in non-green areas remained stable at around 4, reflecting that the temperature heterogeneity of non-green areas is stronger. In addition, there was a significant difference in temperature data between green areas and non-green areas in 2010, which may be related to the climate conditions and data quality of that year.

3.3.2. Buffer Zone Cooling Effect

Related studies have shown that the effective cooling range of green spaces is generally within 500m [11]. Therefore, this study established five buffer zones within a 500m radius outside the green area, with 100m intervals. The average temperature of each buffer zone was overlaid to create line graphs and tables, thereby observing the change of surface temperature with distance. Based on other studies, this study considers the distance from the first inflection point where the temperature increases to decrease to the distance from the green space as the effective cooling distance of the green space, and the slope represents the cooling magnitude.

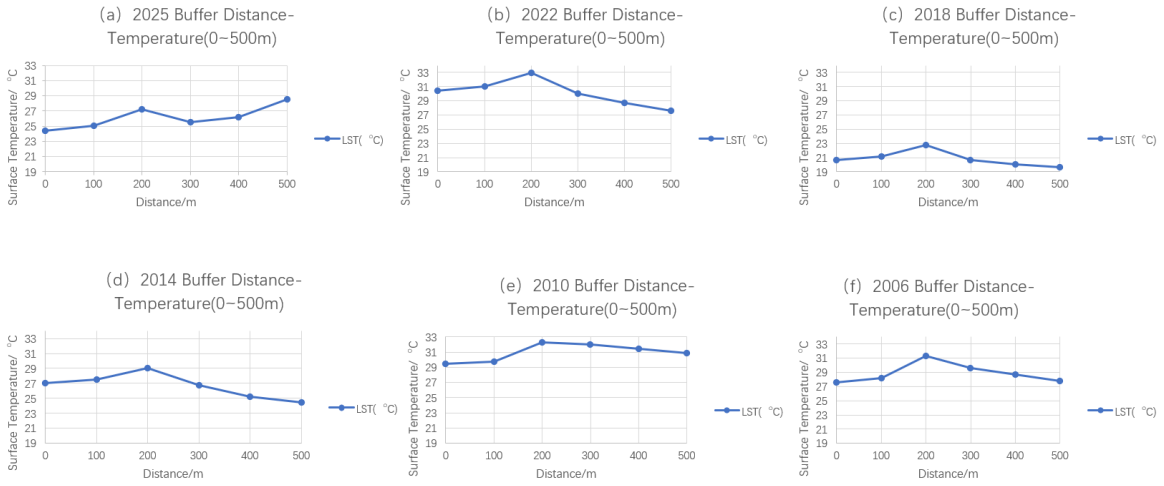


Fig. 5 0-500m Buffers' Distance-Temperature Line Graph

As shown in Fig 5, the ambient temperature around the green space is generally higher than the temperature inside the green space, and within a certain range, the ambient temperature increases with increasing distance. The overall slope changes in a rhythm from high to low, with the temperature inflection point at 200m. The slope of the broken line is the steepest and the change is most significant in the buffer zone from 100m to 200m, the temperature increase within the 0-100m distance does not exceed 1°C. Therefore, it can be seen that between 2006 and 2025, the effective cooling distance of green space is 200m, and the area where the cooling effect is most drastically reduced is between 100m and 200m away from the green space. Moreover, the reason why the temperature dropped instead of rising after 200m may be that the buffer zone encountered water with a lower temperature.

3.4. Pearson Correlation and Linear Regression Model of Green Space Area and LST

To investigate the correlation between the green space in a region and the regional average temperature, this paper will use the Pearson correlation coefficient and construct a linear regression model for measurement. As can be observed from Table 3, from 2014 to 2025, there was an increase in green space area but also an increase in temperature. This situation is likely related to the reduced connectivity of green space and the increased fragmentation. Similarly, the surrounding built-up area environment may also play a potential role in regulating the geothermal environment. Table 4 shows the linear regression model and goodness of fit between green area and average temperature in Guangzhou. The results show that the linear regressive line model has a negative slope (m=-0.0019) and the two have a negative correlation (r=-0.28188), that is, the larger the green area, the lower the

surface temperature. However, the goodness of fit of the linear model is low(R2=0.0795), this coefficient indicates that the model can only explain approximately 7.95% of the surface temperature variation.

Table 3. Green space area and average temperature in Guangzhou

Year	Green spaces area/km^2	Guangzhou average LST/℃
2025	5948.35	25.12
2022	6042.75	31.10
2018	5944.66	21.19
2014	6196.44	27.53
2010	4775.25	29.95
2006	6059.47	28.25

Table 4. Linear fitting formula and degree of fit

Linear regressive line	$y = -0.0019x + 38.454$
Fitness R^2	0.0795

4. Conclusion

Based on Google Earth Engine (GEE) platform and Landsat series satellite remote sensing data (2006-2025), this study constructed a green space distribution map and a city heat island classification map (SUHI) for Guangzhou using the NDVI threshold method (NDVI greater than 0.25) and the mean standard method, respectively. The cooling effect of green space on the surface urban heat island was quantified by buffer analysis and independent samples t test. The study explains the spatial evolution of Guangzhou's thermal environment from 2006 to 2025, including the advanced heat island and the fact that high-temperature areas are mainly concentrated in the urban built-up area, while low-temperature areas are relatively fragmented and concentrated in the north. During the study period, the overall distribution of green space remained stable, with the total area of green space decreasing by 111.12km2 between 2006 and 2025, the area reduced was about 1.8% of the total green space area in 2006, but the overall trend was towards fragmentation, which corresponds to the expansion of the southern heat island and high-temperature areas. In addition, the cooling effect is most obvious at a distance of 0-200m from the green space, and the t-test shows that the surface temperature of the green space is significantly lower than that of the non-green space, this indicates that the spatial pattern of green spaces, rather than simply their total area, has a more critical impact on the urban heat island effect. Compared to highly connected patchy green spaces, fragmented and dispersed green spaces have significantly limited cooling capacity. Furthermore, Pearson correlation coefficient statistics show a negative correlation between green space area and surface temperature (r = -0. 28188), and the linear fit is low(R^2=0.0795), explaining only about 7.95% of the temperature variation, revealing the complexity of the urban thermal environment.

Additionally, this study has the following limitations. First, the presence of missing bands in remote sensing satellite imagery may cause errors in temperature estimation. Secondly, this study did not consider the effects of topography, wind field, and the proportion of impermeable surfaces, and lacked a precise classification of green space types. This explains why the linear model has a low model fit, and also confirms that existing research lacks a comprehensive study that combines satellite remote sensing data and urban meteorological data to further analyze the changes in Guangzhou's heat island effect. Future research could be improved in the following ways: combining machine learning (such as random forests) to classify topography, constructing multivariate nonlinear models to improve model fit and spatial prediction capabilities, and introducing high-precision remote sensing data to more accurately assess the cooling effect of different green spaces.

References

[1] Un-habitat. World Cities Report 2022: Envisaging the Future of Cities [DB/OL], 2022. https://unhabitat.org/world-cities-report-2022-envisaging-the-future-of-cities. [2026-06-05]

[2] Wu, L., Wu, Q. J., Wu, W. Y., et al. (2022). A review of research on spatiotemporal dynamic evolution effects of urban green space based on remote sensing. Journal of Ecology and Environment, 41(4), 42-48.

[3] Zhang Z Y, Paschalis A, Mijic A, et al. A mechanistic assessment of urban heat island intensities and drivers across climates[J]. Urban Climate, 2022, 44: 101215.

[4] Yuan Y, Li C W, Geng X L, et al. Natural-anthropogenic environment interactively causes the surface urban heat island intensity variations in global climate zones[J]. Environment International, 2022, 170: 107574.

[5] Morabito M, Crisci A, Moriondo M, et al. Air temperature-related human health outcomes:

Current impact and estimations of future risks in Central Italy[J]. Science of the Total Environment, 2012, 441: 28-40.

[6] Su, Y. X., Huang, G. Q., Chen, X. Z., et al. (2010). The cooling effect of Guangzhou city parks to surrounding environments. Acta Ecologica Sinica, 30(18), 4905-4918.

[7] Fan, Y. P., Xu, H. Q., Li, L., et al. (2014). Analysis of urban expansion and urban heat island effect in Guangzhou city. Remote Sensing Information, 29(1), 23-29.

[8] Wang, M. Y., & Xu, H. Q. (2021). A comparative study on the changes in heat island effect in Chinese and foreign megacities. Remote Sensing for Natural Resources, 33(4), 200-208.

[9] Ru, H., Chen, Q., Jin, X. J., Zhang, X. T., Gou, J. J., & Lu, R. H. (n.d.). The regulatory effect of blue-green space on urban heat islands. Chinese Urban Forestry. [Online].

[10] Liu, G. L., Huang, Z. X., Zhang, L. S., et al. (2022). Study on the impact of urban greenspace on urban heat island effect in Nanchang City. Jiangxi Science, 44(2), 348-357. DOI:10.13990/j.issn1001-3679.2026.02.021.

[11] Wang, Y. X., Dong, J. W., Wang, Y. Z., et al. (2005). Discussion on the relationship between urban green space and urban heat island effect. Subtropical Plant Science, 34(4), 55-59.

[12] Liu, F. F., & Xu, H. Q. (2024). Study on the evolution of the urban thermal environment ofGuangzhou by coupling satellite thermal infrared imagery with meteorological data. Remote

[13] USGS. USGS Landsat 5 Level 2, Collection 2, Tier 1. 1984-01-01. Cited 2026-06-15. https://developers.google.com/earth-engine/datasets/catalog/LANDSAT_LT05_C02_T1_L2

[14] USGS. USGS Landsat 8 Level 2, Collection 2, Tier 1. 2013-01-01. Cited 2026-06-15. https://developers.google.com/earth-engine/datasets/catalog/LANDSAT_LC08_C02_T1_L2

[15] USGS. USGS Landsat 9 Level 2, Collection 2, Tier 1.2021-01-01. Cited 2026-06-15. https://developers.google.com/earth-engine/datasets/catalog/LANDSAT_LC09_C02_T1_L2